

Probing Hidden Orders with Resonant Inelastic X-Ray Scattering

Lucile Savary and T. Senthil

Department of Physics, Massachusetts Institute of Technology, 77 Massachusetts Ave., Cambridge, MA 02139

(Dated: July 14, 2021)

We propose a general scheme for the derivation of the signals resonant inelastic (and elastic) x-ray scattering (RIXS) gives access to. In particular, we find that RIXS should allow to directly detect many hidden orders, such as spin nematic, bond nematic, vector and scalar spin chiralities. To do so, we choose to take the point of view of effective operators, leaving microscopic details unspecified, but still keeping experimentally-controllable parameters explicit, like the incoming and outgoing polarizations of the x-rays. We ask not what microscopic processes can lead to a specific outcome, but, rather, what couplings are in principle possible. This approach allows to systematically enumerate all possible origins of contributions to a general RIXS signal. Although we mainly focus on magnetic insulators, for which we give a number of examples, our analysis carries over to systems with charge and other degrees of freedom, which we briefly address. We hope this work will help guide theorists and experimentalists alike in the design and interpretation of RIXS experiments.

I. INTRODUCTION

Many systems have ground states with well-defined order parameters which couple directly to conventional probes such as neutrons or light. The accessible data usually comes in the form of “structure factors,” i.e. correlation functions of two “elementary” observables. Classic examples are magnetically ordered states, e.g. ferromagnets and antiferromagnets whose magnetic structure and fluctuations can be resolved by methods like neutron scattering, muon spin resonance (μ SR), nuclear magnetic resonance (NMR) etc.. However, many of the “exotic” phases proposed by theorists do not fall into this category. Some states exist, for example, which possess a well-defined local order parameter, but still evade robust characterization using “conventional” probes. The order is then commonly referred to as “hidden.” Typically, the order parameters of such systems have quantum numbers which are multiples of those which elementary particles give access to when coupled linearly to the system. For example neutrons can excite $S = 1$ magnons, but not $S = 2$ excitations (owing to the dipolar coupling between the neutron and electron’s spins). Perhaps the simplest and best-known example of a hidden order is that of spin quadrupolar (also called nematic) order [1]. In that case, the expectation values of the spin projections, $\langle S_i^\mu \rangle$ (note the spins transform as “dipoles”) are zero, but those of “quadrupolar” operators, like $\langle S_i^\mu S_i^\nu \rangle$, are not. Many other types of hidden orders have been proposed in the literature. Among those are spin “bond nematic” [2, 3], where the order parameter contains spins on neighboring sites, and spin vector and scalar chiralities, which involve antisymmetric products of spins. Hidden orders also arise in conducting systems, with the famous example of nematic (in that case, “nematic” refers to rotation –discrete or continuous– symmetry breaking in real space) order in the pnictide superconductors.

Here we show that Resonant Elastic and Inelastic X-Ray Scattering (REXS and RIXS) can in principle measure spin nematic, vector and scalar chirality, and many more correlation functions (static and dynamical for

REXS and RIXS, respectively). In general, we propose an enveloping scheme which allows to systematically enumerate which correlation functions will contribute to the RIXS signal in any given polarization geometry. REXS signals are obtained from RIXS in the $\omega \rightarrow 0$ limit. In particular, in the case of static order, REXS signal should display corresponding “Bragg” peaks.

“Resonant scattering” refers to techniques where the energy of an incoming probe is tuned to a “resonance” (a.k.a. “edge”). In that case, not only is the absorption (virtual or real) cross-section dramatically enhanced, but the latter may also involve nontrivial operators, allowing to probe correlation functions of complex order parameters, i.e. typically those of hidden orders, which are otherwise hardly accessible. This is clear upon thinking in terms of perturbation theory in the probe-system coupling amplitude, and we soon specialize to an x-ray probe. The scattering amplitude up to second order is given by [4, 5]

$$\mathcal{T}_{\mathbf{f}\mathbf{i}} = \langle \mathbf{f} | \hat{H}' | \mathbf{i} \rangle + \sum_n \frac{\langle \mathbf{f} | \hat{H}' | n \rangle \langle n | \hat{H}' | \mathbf{i} \rangle}{E_{\mathbf{i}} - E_n}, \quad (1)$$

where $|\mathbf{i}, \mathbf{f}\rangle$ denote the initial and final states of the {system + electromagnetic (EM) field}, \hat{H}' is the coupling Hamiltonian between matter and the EM field, $\{|n\rangle\}$ forms a complete set of states (the “important” ones will be discussed later) of the system, and E_α is the energy of the state $|\alpha\rangle$. When there exist states $|n\rangle$ which are close in energy to $E_{\mathbf{i}}$, the system is said to be at resonance with the probe and the second order amplitude in Eq. (1) largely dominates the first. Moreover, within perturbation theory, the former contains, among others, the following chain of (virtual) processes: the absorption of a photon, the evolution of the resulting system, followed by the emission of a photon. The RIXS signal is the cross-section relative to the amplitude of such a process, when the incoming x-ray light is tuned to a resonance which involves the excitation of a core electron to a valence level, i.e. when $|n\rangle$ is a state of the pure system (no photons) and contains a “core hole”. Typical orders of

magnitude for such x-ray frequencies range between 0.01 and 10 keV [5–7], i.e. correspond to photon wavevectors of order $1\text{-}10^{-3} \text{ \AA}^{-1}$.

Detailed microscopic analyses of RIXS processes in a number of systems have been described at length in the literature [5], some even predicting the observation of correlation functions of complex order parameters [8, 9]. Here we do not belabor on them, but rather base the analysis entirely on the observation that the initial (before the photon is absorbed) and final states (after the photon is emitted) of the system both belong to its low-energy manifold. Essentially, in that approach, the only important feature of the microscopics is the reduction of (at least spatial) symmetries to those of the core-hole site point group. Such a symmetry-based strategy has a few major advantages. An accurate description of all possible microscopic processes is a very complex many-body problem, which is moreover subjected to many uncertainties concerning the atomic structure in a material. As a consequence, such approaches are inherently material-specific. It is moreover very difficult to exhaust all possible processes through microscopic reasoning. The symmetry procedure bypasses these issues. This type of *fully* effective approach was recently insightfully pioneered in Ref. 10 in the context of magnetic insulators, where the author gave the form of on-site effective RIXS operators for up to two on-site spin operators. Here we constructively rederive and generalize Ref. 10’s main result to all possible symmetry-allowed couplings, including those which involve multiple-site operators and degrees of freedom other than just spins. Moreover, the broader context of the derivation presented here helps make more transparent the correlations possibly probed in RIXS, on which we focus.

The remainder of this paper is organized as follows. We first review the form of the light-matter interaction, the important symmetries to be considered, and derive the form of the effective operators whose correlations RIXS measures in insulating magnetic systems, which are summarized in Table I. We then turn to the study of three important examples of hidden orders as may be realized in real materials: spin nematic order, bond nematic order, vector and scalar chiralities, and calculate the expected RIXS signals in these three concrete cases. At the end of the paper we briefly address systems with charge degrees of freedom.

II. EFFECTIVE OPERATORS

The leading order Hamiltonian \hat{H}' which couples light to matter and is involved in the *second*-order amplitude of the interaction cross-section is given by, in the Coulomb gauge $\nabla \cdot \mathbf{A} = 0$ [5][11]:

$$\hat{H}' = \sum_{\mathbf{r}} \left[\hat{\psi}_{\mathbf{r}}^{\dagger} \frac{e\mathbf{p}}{m} \hat{\psi}_{\mathbf{r}} \cdot \hat{\mathbf{A}}_{\mathbf{r}} + \hat{\psi}_{\mathbf{r}}^{\dagger} \frac{e\hbar\boldsymbol{\sigma}}{2m} \hat{\psi}_{\mathbf{r}} \cdot (\nabla \times \hat{\mathbf{A}}_{\mathbf{r}}) \right], \quad (2)$$

with the vector potential

$$\hat{\mathbf{A}}_{\mathbf{r}} = \sum_{\mathbf{k}} \sqrt{\frac{\hbar}{2V\epsilon_0\omega_{\mathbf{k}}}} \sum_{\boldsymbol{\varepsilon}} \left(\boldsymbol{\varepsilon}^* \hat{a}_{\mathbf{k},\boldsymbol{\varepsilon}}^{\dagger} e^{-i\mathbf{k}\cdot\mathbf{r}} + \text{h.c.} \right). \quad (3)$$

\hat{H}' acts in the product space of the electrons \mathcal{H}_{e-} and photons $\mathcal{H}_{\text{phot}}$, $\mathcal{H} = \mathcal{H}_{e-} \times \mathcal{H}_{\text{phot}}$, $\hat{\psi}^{\dagger}$ and $\hat{\psi}$ are the electron creation and annihilation second-quantized operator fields, \hbar is Planck’s constant over 2π , e and m are the electron charge and mass, respectively, \hat{a}^{\dagger} and \hat{a} are the photon creation and annihilation operators, $\boldsymbol{\varepsilon}$ denotes the photon polarization, V is the volume in which the EM field is enclosed, ϵ_0 is the dielectric polarization of vacuum and $\omega_{\mathbf{k}} = \omega_{-\mathbf{k}} = c|\mathbf{k}|$ where c is the speed of light. Here, for concreteness, we make two approximations, often used in the literature [5]: we consider (i) that $|\mathbf{k} \cdot \delta\mathbf{r}| \ll 1$ at the relevant x-ray wavelengths, where $\mathbf{r} = \mathbf{R} + \delta\mathbf{r}$ where \mathbf{R} denotes the position of a lattice site, and so, at zeroth order, $e^{i\mathbf{k}\cdot\delta\mathbf{r}} \approx 1$ [12], and (ii) that in Eq. (2) the magnetic term ($\propto \boldsymbol{\sigma}$) is subdominant compared to the “electric” one ($\propto \mathbf{p}$). We return to these approximations in Appendix E. Therefore, the second-order RIXS amplitude for processes with a core hole at site \mathbf{R} reduces to

$$\begin{aligned} \mathcal{T}_{\mathbf{R}}^{\text{if}} &= \sum_{\mathbf{q}, \mathbf{q}', \boldsymbol{\varepsilon}, \boldsymbol{\varepsilon}'} \left\langle \mathbf{f} \left| \left[\boldsymbol{\varepsilon}' \hat{a}_{\mathbf{q}'} e^{i\mathbf{q}'\cdot\mathbf{R}} + \boldsymbol{\varepsilon}'^* \hat{a}_{\mathbf{q}'}^{\dagger} e^{-i\mathbf{q}'\cdot\mathbf{R}} \right] \right. \right. \\ &\quad \left. \left. \times \hat{\mathcal{O}}_{\mathbf{R}} \left[\boldsymbol{\varepsilon} \hat{a}_{\mathbf{q}} e^{i\mathbf{q}\cdot\mathbf{R}} + \boldsymbol{\varepsilon}^* \hat{a}_{\mathbf{q}}^{\dagger} e^{-i\mathbf{q}\cdot\mathbf{R}} \right] \right| \mathbf{i} \right\rangle \\ &= \mathcal{A}_{\mathbf{k}, \mathbf{k}'} \left\langle \mathbf{f} \left| \boldsymbol{\varepsilon}'^* \hat{\mathcal{O}}_{\mathbf{R}}^{\mu\nu} \boldsymbol{\varepsilon}_{\nu} \right| \mathbf{i} \right\rangle e^{i(\mathbf{k}-\mathbf{k}')\cdot\mathbf{R}}, \end{aligned} \quad (4)$$

where $\hat{\mathcal{O}} \sim \frac{1}{\sqrt{\omega_{\mathbf{q}}\omega_{\mathbf{q}'}}} \mathbf{p} \hat{G} \mathbf{p}$, with $\hat{G} = \sum_n \frac{|n_{\mathbf{R}}\rangle \langle n_{\mathbf{R}}|}{E_i + \hbar\omega_{\mathbf{q}} - E_n}$, where $|n\rangle$ are restricted to “intermediate” states with a core hole at site \mathbf{R} (i.e. close to resonance). The second expression Eq. (5) is obtained by requiring $|\mathbf{i}\rangle = |\mathbf{i}\rangle \otimes |\mathbf{k}\boldsymbol{\varepsilon}\rangle$ and $|\mathbf{f}\rangle = |\mathbf{f}\rangle \otimes |\mathbf{k}'\boldsymbol{\varepsilon}'\rangle$. Importantly, $\hat{\mathcal{O}}$ acts purely in electronic space, and moreover *within the low-energy manifold*, provided the system immediately “returns” to a low-energy state as the outgoing photon is emitted, as is usually assumed. We therefore ask: what effective operator acts purely in this manifold which reproduces the matrix elements $\mathcal{T}_{\mathbf{R}}^{\text{if}}$? If we know the low-energy manifold and a basis which spans it, and if the basis elements are physically meaningful, we shall immediately obtain which correlation functions RIXS produces. We insist once again that, within this approach, all “intermediate processes,” no matter how complicated, are in a sense included, and need not be discussed.

As usual, most general arguments stem from symmetry considerations, which we now address. The core hole is immobile, which imposes a strong symmetry constraint on $\hat{\mathcal{O}}_{\mathbf{R}}$: it should be invariant in real space under point (site \mathbf{R}) group symmetries. Another constraint comes from the “locality” of the effect of the core-hole in the “intermediate propagation time” $\tau = 1/\Gamma \sim 10^{-15} \text{ s}$ [5], which implies that only operators which act in close proximity to the site of the core hole should be involved.

While this statement may appear somewhat loose, a quick order-of-magnitude analysis shows that, *even in a metal*, electrons will not travel over more than very few lattice spacings over the time τ [13]. Finally, since transition amplitudes are scalars, by keeping the polarization dependence explicit, we impose constraints on the combination of operators which multiply the polarization components. This is what we address now and is summarized in Table I.

For concreteness and ease of presentation of the derivation we now focus on magnetic insulators, though we note that the same ideas carry over to systems with charge (and other) degrees of freedom, to which we return at the end of the paper, in Sec. V. Indeed, because of the “locality” of the effective scattering operators, insulating systems are more readily tackled. Local (in the sense of acting only on degrees of freedom living in a small neighborhood in real space) operators in insulating systems yield a very natural description of the system, and the low-energy manifold, being finite (generally a well-defined J multiplet, possibly split by crystal fields) and sharply defined (usually a gap separates multiplets), can be spanned by effective “spin” operators (finite vector spaces of identical dimensions are isomorphic). Therefore only a spin operator basis compatible with the combinations of polarizations remains to be found.

In the absence of both spin-orbit coupling *at low energies* (core levels always experience very strong spin-orbit coupling [5]) and of a magnetic field, the system should be rotationally symmetric in spin space. Moreover, in principle, in the Hamiltonian, under spatial symmetries, the spins are left invariant. However, here, in the RIXS structure factor, the situation is more subtle. Spin excitations (and hence spin operators) may only arise in the structure factor thanks to spin-orbit coupling at the core. Therefore, in principle the structure factor itself should display signs spin-orbit coupling [10, 14], with the effective spin operators transforming under *lattice* symmetries. Even upon neglecting transition operators which break rotational symmetry if spin orbit coupling is weak at the valence level, the effective spins still transform under *real space* symmetry operations.[15] Then, the polarizations and (effective) spins (the latter make up the operators $\hat{O}^{\mu\nu}$, as mentioned above) transform as usual vectors and pseudo-vectors, respectively, under spatial transformations, and according to $\boldsymbol{\varepsilon} \rightarrow -\boldsymbol{\varepsilon}^*$ and $\mathbf{S} \rightarrow -\mathbf{S}$ under time reversal (see Appendix B). In other words, under the full spherical symmetry group, using the notations from Ref. 16, $\boldsymbol{\varepsilon}$ and \mathbf{S} transform under D_1^- and D_1^+ , respectively (under $SO(3)$ operations, both the polarization and spin vectors transform under the $L = 1$ representation). Since $D_1^\pm \times D_1^\pm = D_0^+ + D_1^+ + D_2^+$ ($1 \times 1 = 0 + 1 + 2$ for $SO(3)$), *any* combination of spin operators which transform under the same representations can in principle be involved in the RIXS signal. Depending on the number of neighboring operators one chooses to include (and on the value of $S(S + 1)$), possibilities differ. The situation for up to three spin operators (on

the same or nearby sites, from “locality”) is summarized in Table I (see in particular the caption), and details of the derivation are given in Appendix C.

On-site terms.— Upon considering on-site terms only ($i = j = k$), where one need not take into account any further lattice symmetries, and *up to two* spin operators, we recover the expression from Ref. 10:[17]

$$T_i = \alpha_0(\boldsymbol{\varepsilon}'^* \cdot \boldsymbol{\varepsilon}) + \alpha_1(\boldsymbol{\varepsilon}'^* \times \boldsymbol{\varepsilon}) \cdot \mathbf{S}_i + \alpha_2[\boldsymbol{\varepsilon}'^*, \boldsymbol{\varepsilon}][\mathbf{S}_i, \mathbf{S}_i], \quad (6)$$

where $T_i = \boldsymbol{\varepsilon}'^* \mathcal{O}_i^{\mu\nu} \boldsymbol{\varepsilon}_\nu$, and where $[\mathbf{S}_i, \mathbf{S}_j]$ is the traceless symmetric second rank tensor constructed from \mathbf{S}_i and \mathbf{S}_j , i.e. given by: $[\mathbf{S}_i, \mathbf{S}_j]_{\mu\nu} = \frac{1}{2}(S_i^\mu S_j^\nu + S_i^\nu S_j^\mu) - \frac{1}{3}(\mathbf{S}_i \cdot \mathbf{S}_j)\delta_{\mu\nu}$, and analogously for $[\boldsymbol{\varepsilon}'^*, \boldsymbol{\varepsilon}]$. The symmetric product $[\boldsymbol{\varepsilon}'^*, \boldsymbol{\varepsilon}][\mathbf{S}_i, \mathbf{S}_i] = \sum_{\mu,\nu} [\boldsymbol{\varepsilon}'^*, \boldsymbol{\varepsilon}]_{\mu\nu} [\mathbf{S}_i, \mathbf{S}_i]_{\mu\nu}$ has all indices contracted. The α_n are material-specific coefficients [10]. The generalization to discrete symmetries is *formally* straightforward (though usually gruesome in practice) and discussed in detail in Appendix D.

Off-site terms.— The above considerations take care of the symmetry aspects relative to spin space. To fulfill the constraints associated with the lattice, which enters through $\mathbf{S}_\mathbf{r} \rightarrow [\det R] R \cdot \mathbf{S}_{R\cdot\mathbf{r}}$ where R is a spatial operation (see Appendix B), the expressions must be appropriately symmetrized. For example, take a 1d chain of $S = 1/2$, and consider a maximum of two spin terms. Then, if lattice sites are centers of inversion, the transition operator will be (still assuming spherical symmetry in spin space):

$$\begin{aligned} T_i &= \alpha_0(\boldsymbol{\varepsilon}'^* \cdot \boldsymbol{\varepsilon})\mathbf{S}_i \cdot (\mathbf{S}_{i-1} + \mathbf{S}_{i+1}) \\ &\quad + (\boldsymbol{\varepsilon}'^* \times \boldsymbol{\varepsilon}) \cdot (\alpha_{1,1}\mathbf{S}_i + \alpha_{1,2}\mathbf{S}_i \times (\mathbf{S}_{i-1} + \mathbf{S}_{i+1})) \\ &\quad + \alpha_2[\boldsymbol{\varepsilon}'^*, \boldsymbol{\varepsilon}][\mathbf{S}_i, \mathbf{S}_{i-1} + \mathbf{S}_{i+1}], \end{aligned} \quad (7)$$

where the α_n and $\alpha_{n,m}$ are material-specific coefficients which multiply terms which belong to the same irreducible representation (n) (or copy (m) thereof if an irreducible representation appears multiple times).

From Table I, one may directly read out the quantities whose correlation functions will contribute to the RIXS signal, as well as which polarization geometry will reveal them while switching off (most of) the other contributions (e.g. $\boldsymbol{\varepsilon}'^* \parallel \boldsymbol{\varepsilon}$ will “switch off” the $\boldsymbol{\varepsilon}'^* \times \boldsymbol{\varepsilon}$ “channel”). Indeed the differential cross-section is given by [4]

$$\begin{aligned} &\frac{\delta^2 \sigma}{\delta \Omega \delta E} \\ &\propto \sum_f \left| \sum_{\mathbf{R}, \mathbf{q}} \langle f | T_{\mathbf{q}} | i \rangle e^{i(\mathbf{q} + \mathbf{k} - \mathbf{k}') \cdot \mathbf{R}} \right|^2 \delta(E_f + \omega_{\mathbf{k}'} - E_i - \omega_{\mathbf{k}}) \\ &\propto \sum_{\mathbf{q}} \langle i | T_{-\mathbf{q}} T_{\mathbf{q}} | i \rangle \delta(\mathbf{q} + \mathbf{k} - \mathbf{k}') \delta(\Delta E - \omega_{\mathbf{q}}), \end{aligned} \quad (8)$$

where $\delta \Omega$ and δE denote elementary solid angle (related to the momentum transfer $\widehat{\mathbf{k} - \mathbf{k}'}$) and energy, respectively, and where ΔE is the measured energy transfer.

Before moving on to the discussion of specific examples, we make a couple of important remarks. (i) It is

representation	polarizations	one spin	two spins	three spins
0	$\boldsymbol{\varepsilon}'^* \cdot \boldsymbol{\varepsilon}$		$\mathbf{S}_i \cdot \mathbf{S}_j$	$(\mathbf{S}_i \times \mathbf{S}_j) \cdot \mathbf{S}_k$
1	$\boldsymbol{\varepsilon}'^* \times \boldsymbol{\varepsilon}$	\mathbf{S}_i	$\mathbf{S}_i \times \mathbf{S}_j$	$(\mathbf{S}_i \cdot \mathbf{S}_j) \mathbf{S}_k, (\mathbf{S}_i \times \mathbf{S}_j) \times \mathbf{S}_k, \llbracket \mathbf{S}_i, \mathbf{S}_j \rrbracket \cdot \mathbf{S}_k$
2	$\llbracket \boldsymbol{\varepsilon}'^*, \boldsymbol{\varepsilon} \rrbracket$		$\llbracket \mathbf{S}_i, \mathbf{S}_j \rrbracket$	$\llbracket \mathbf{S}_i \times \mathbf{S}_j, \mathbf{S}_k \rrbracket, \llbracket \mathbf{S}_i, \mathbf{S}_j \rrbracket \times \mathbf{S}_k$

TABLE I. *Generic* form of the operators in magnetic systems which couple to combinations of the polarizations in the absence of spin-orbit coupling. The double brackets represent the traceless symmetric products, $\llbracket \mathbf{u}, \mathbf{v} \rrbracket_{\mu\nu} = \frac{1}{2}(u^\mu v^\nu + u^\nu v^\mu) - \frac{1}{3}(\mathbf{u} \cdot \mathbf{v})\delta_{\mu\nu}$, and the dot and vector products between a matrix (obtained through $\llbracket \cdot, \cdot \rrbracket$) and a vector are defined such that: $(\llbracket \mathbf{u}, \mathbf{v} \rrbracket \cdot \mathbf{w})_\mu = \sum_\nu \llbracket \mathbf{u}, \mathbf{v} \rrbracket_{\mu\nu} w_\nu$, $(\llbracket \mathbf{u}, \mathbf{v} \rrbracket \times \mathbf{w})_{\mu\rho} = \sum_{\nu,\lambda} \epsilon_{\nu\lambda\rho} \llbracket \mathbf{u}, \mathbf{v} \rrbracket_{\mu\nu} w_\lambda$ (see Appendix C). Moreover, the product $\llbracket \mathbf{u}, \mathbf{v} \rrbracket \llbracket \mathbf{w}, \mathbf{t} \rrbracket$ also denoted $\llbracket \mathbf{u}, \mathbf{v} \rrbracket \cdot \llbracket \mathbf{w}, \mathbf{t} \rrbracket$ is defined to be the fully symmetric product with all indices contracted: $\sum_{\mu\nu} \llbracket \mathbf{u}, \mathbf{v} \rrbracket_{\mu\nu} \llbracket \mathbf{w}, \mathbf{t} \rrbracket_{\mu\nu}$. Each row corresponds to a given irreducible representation of a combination of the incoming and outgoing polarization, given in the second column. Each entry on the right of the double bar gives the combinations of spins which transform as does the combination of polarizations on the same line. The columns simply indicate the number of spin operators involved in the effective operator. In principle, RIXS may measure correlations functions of the operators given in this table. This table is also “valid” for matrices which connect local “band” indices with the same symmetries in conducting systems. See Sec. VI.

important to note that, for effective spin-1/2 systems, only off-site terms can contribute to, for example, the $\llbracket \boldsymbol{\varepsilon}'^*, \boldsymbol{\varepsilon} \rrbracket$ channel. Indeed, there exist only four (counting the identity) linearly independent $S = 1/2$ operators. Therefore, while off-site contributions are expected to be weaker (they may only arise from so called “indirect” processes [5]), in an effective $S = 1/2$ system, a “multi-site” signal in the $\llbracket \boldsymbol{\varepsilon}'^*, \boldsymbol{\varepsilon} \rrbracket$ channel will not “compete” with signal from possibly-larger onsite couplings, offering hope to unambiguously detect such correlations. (ii) We caution that, of course, this symmetry-based approach does not any give information on the absolute or relative strengths of the signals in the different channels. Moreover, “selection rules” relative to the chosen “edge” need to be additionally taken into account. (iii) An additional word of caution is in order: as far as we understand, the measurement of the *outgoing* polarization is not currently possible on instruments being used at this point, although the new state-of-the art facility currently under construction (which will also provide much higher resolution in energy, currently at around 100 meV) will be able to.

III. SPIN NEMATIC IN THE BILINEAR-BIQUADRATIC $S = 1$ MODEL ON THE TRIANGULAR LATTICE

The $S = 1$ bilinear biquadratic model with Hamiltonian

$$H = \sum_{\langle i,j \rangle} (J_1 \mathbf{S}_i \cdot \mathbf{S}_j + J_2 (\mathbf{S}_i \cdot \mathbf{S}_j)^2), \quad (9)$$

on the triangular lattice has been quite intensively studied, especially so in recent years after it was suggested that it could be relevant to the insulating material NiGa_2S_4 , where Ni^{2+} is magnetic, with $S = 1$ [18–23]. This material is made of stacked triangular planes of Ni^{2+} ions, and displays no long-range spin ordering but low-temperature specific heat which grows with temperature as T^2 [18]. The latter facts motivated the

minimal description of NiGa_2S_4 by the model Eq. (9), which, for $J_1 > 0$, features two quadrupolar phases, one “ferroquadrupolar” and one “antiferroquadrupolar.” These phases are characterized by a vanishing expectation value for the spins, $\langle S_i^\mu \rangle = 0$, but an on-site “quadrupolar” (a.k.a. “spin nematic”) order parameter: $\langle \{S_i^\mu, S_i^\nu\} - 2\delta_{\mu\nu} \rangle \neq 0$ (a diagonal part is subtracted to obtain a traceless operator). Since here we look not to accurately make predictions for the actual material NiGa_2S_4 , but rather to demonstrate that RIXS will provide unambiguous signatures of quadrupolar order, we now restrict our attention to the minimal bilinear-biquadratic model Eq. (9), despite the fact that the latter will clearly not account for all the experimental features (not discussed here) of NiGa_2S_4 [22].

The wavefunctions of nematic states are simple single-site product wavefunctions. For spin-1 systems, product wavefunctions can generally be expressed as $|\psi\rangle = \prod_i \mathbf{d}_i \cdot |\mathbf{r}_i\rangle$, where we have defined $|\mathbf{r}_i\rangle = (|x_i\rangle, |y_i\rangle, |z_i\rangle)$, where $\mathbf{d}_i \in \mathbb{C}^3$ and $|\mathbf{d}_i| = 1$. The states $|\mu_i\rangle$ are time-reversal invariant states defined such that $S_i^\mu |\mu_i\rangle = 0$, i.e., in terms of the usual eigenstates of the S_i^z operator, $|x\rangle = \frac{i}{\sqrt{2}}(|1\rangle - |\bar{1}\rangle)$, $|y\rangle = \frac{1}{\sqrt{2}}(|1\rangle + |\bar{1}\rangle)$ and $|z\rangle = -i|0\rangle$ [24]. In the case of a “pure” quadrupolar phase, for this basis choice (with time-reversal invariant states), $\mathbf{d}_i \in \mathbb{R}^3$ [24], which one can check indeed leads to $\langle \mathbf{S}_i \rangle = \mathbf{0}$. The vector \mathbf{d}_i at each site is called the “director,” and corresponds to the direction along which the spins do *not* fluctuate. In nematic states, the direction along which the director points may vary at each site, like in the “antiferroquadrupolar” phase of the above model, where the *directors* form a three-sublattice 120° configuration. In the ferroquadrupolar phase, the directors on each site point in the same direction, which can be arbitrarily (since the Hamiltonian is isotropic in spin space) taken to be the z direction. In that case, the unit cell is not enlarged. In ordered (or field-polarized) ferromagnets and antiferromagnets, the low-energy elementary excitations of the system are spin flips/waves, i.e. $S^z = \pm 1$ local excitations. In nematic states, where it is the directors which

are ordered, spin waves translate to “flavor waves” where there are now two pairs of conjugate “transverse” bosons. Flavor wave spectra and dipolar and quadrupolar correlations for the model Eq. (9) on the triangular lattice have been calculated in several references [1, 20, 25, 26]. Our derivation is provided in Appendix F 1, and here we give the full RIXS structure factor for the model, assuming on-site spin operators only (expected to provide the largest contributions to the signal), and spherical symmetries (a derivation is provided in Appendix D), and provide a few plots in Figure 1 for various polarization geometries and assumptions on relative absorption coefficients (about which symmetry analysis gives no further information).

$$\mathcal{I}_{\omega, \mathbf{q}}^{\text{RIXS}} \propto \sqrt{\frac{A_{\mathbf{q}}^2}{A_{\mathbf{q}}^2 - B_{\mathbf{q}}^2}} \left[\left(\kappa_{xy}^{(2)2} + \kappa_{yz}^{(2)2} \right) \left(1 - \frac{B_{\mathbf{q}}}{A_{\mathbf{q}}} \right) + \left(\kappa_z^{(1)2} + \kappa_x^{(1)2} \right) \left(1 + \frac{B_{\mathbf{q}}}{A_{\mathbf{q}}} \right) \right] \delta(\omega - \omega_{\mathbf{q}}), \quad (10)$$

where $A_{\mathbf{q}} = \frac{1}{2}(J_1\gamma_{\mathbf{q}} - 6J_2)$, $B_{\mathbf{q}} = \frac{\gamma_{\mathbf{q}}}{2}(J_2 - J_1)$, $\omega_{\mathbf{q}} = 2\sqrt{A_{\mathbf{q}}^2 - B_{\mathbf{q}}^2}$ with $\gamma_{\mathbf{q}} = 2(\cos q_1 + \cos(\frac{1}{2}[q_1 + \sqrt{3}q_2]) + \cos(\frac{1}{2}[q_1 - \sqrt{3}q_2]))$ and $\kappa_{\mu}^{(1)} = \alpha_1 \epsilon_{\mu\lambda\rho} \epsilon^{\lambda} \epsilon'^{\mu\rho}$ (ϵ is the second rank fully antisymmetric tensor), $\kappa_{\mu\nu}^{(2)} = \alpha_2(-2/3\delta_{\mu\nu}(\epsilon'^{\mu*} \cdot \epsilon) + \epsilon'^{\mu*} \epsilon^{\nu} + \epsilon^{\mu*} \epsilon'^{\nu})$ (note that α_1 and α_2 depend, in particular, on the details of the atomic and crystal structures [10]), see Appendix F 1. Quadrupolar correlations are therefore *directly* seen. Clearly, one recovers the proper scaling of the amplitudes for the Goldstone mode (the system spontaneously breaks spin-rotation symmetry in the ferroquadrupolar phase) at $\mathbf{q} = \mathbf{0}$ at low energy, $\omega_{\mathbf{q}} \sim |\mathbf{q}|$ and $\mathcal{I}^{\text{RIXS, ferro}} \sim 1/\omega_{\mathbf{q}}$. Figure 1 illustrates the associated smoking gun evidence for quadrupolar order provided by RIXS.

IV. BOND NEMATIC AND VECTOR CHIRALITY IN NEAREST AND NEXT-NEAREST NEIGHBOR $S = 1/2$ HEISENBERG CHAINS IN A FIELD

The $S = 1/2$ ferromagnetic nearest-neighbor and antiferromagnetic next-nearest-neighbor Heisenberg model on a chain

$$H = \sum_i (-J_1 \mathbf{S}_i \cdot \mathbf{S}_{i+1} + J_2 \mathbf{S}_i \cdot \mathbf{S}_{i+2} - h S_i^z) \quad (11)$$

with $J_{1,2} > 0$ is thought to be a minimal model for LiCuVO_4 , a distorted “inverse spinel” (with chemical formula $\text{ABB}'\text{O}_4$) material such that the system can be seen in a first approximation as a set of parallel edge-shared CuO_2 chains separated by Li and V atoms [27–29]. Cu^{2+} are magnetic ions with spin $1/2$. As will be important later, we note that the point group symmetry at each Cu site contains inversion symmetry. This material displays a complex phase diagram, which is now believed to

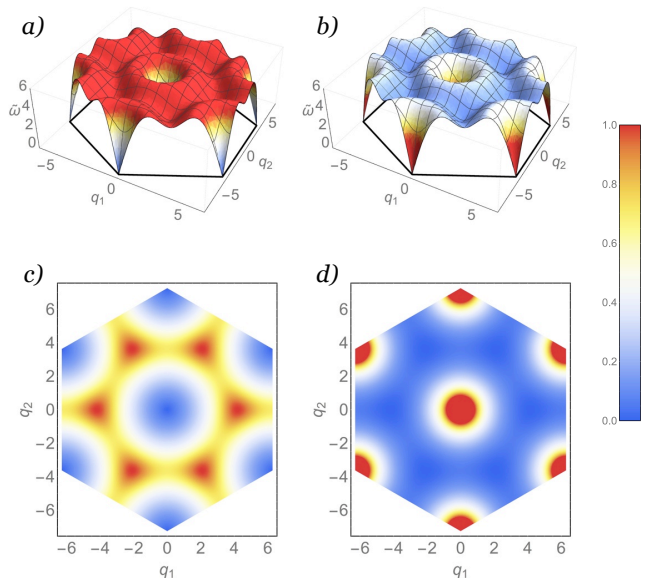


FIG. 1. Color plots of the a) spin-spin correlation function (as probed by e.g. inelastic neutron scattering or RIXS with $\epsilon'^{\mu*} \perp \epsilon$ and α_2 small enough), and b) signal probed by RIXS for $\epsilon = (i, 1, 0)/\sqrt{2}$ and $\epsilon' = (1, i, 0)/\sqrt{2}$, both for the model of Eq. (9) with $J_2/J_1 = -\tan(7\pi/16)$ (ferroquadrupolar phase [20]) on the triangular lattice. c) and d) Equal time (integrated over frequency) versions of the signals shown on plots a) and b), respectively. Note that the intensities are *independently* normalized. On figure b), the intensity is seen to diverge at the Goldstone mode, in sharp contrast with the vanishing of the spin-spin correlation function at the same point in figure a). In plots a) and b), $\tilde{\omega} = \omega/\sqrt{J_1^2 + J_2^2}$.

show, from low to high field: incommensurate helical order, spin density wave order along the chains, and, possibly, right below the saturation field, a spin nematic state. Why the $J_1 - J_2$ Heisenberg model of Eq. (11) seems like a reasonable starting point to describe this material may be articulated as follows: (i) there is experimental evidence for chain structure physics (see above), (ii) Cu usually displays weak spin orbit coupling, suppressing any strong anisotropy in spin space, and (iii) further-neighbor interactions in such compounds are usually sizable, owing to the configurations of the exchange paths. In fact, J_1 and J_2 were estimated to be 19 K and 44 K, respectively, using neutron diffraction and susceptibility data on single crystals [27, 30]. Moreover, in some parameter regime, a number of the phases numerical simulations obtain for the model are reminiscent of those experimentally observed in LiCuVO_4 , as we now discuss.

For $J_2/J_1 > 1/4$, in a non-zero but weak enough field, the minimal *model* has been shown to exhibit a nonzero vector spin chirality $\hat{\mathbf{z}} \cdot \chi_{i,i+1} = \hat{\mathbf{z}} \cdot (\mathbf{S}_i \times \mathbf{S}_{i+1})$ and $\hat{\mathbf{z}} \cdot \chi_{i,i+2} = \hat{\mathbf{z}} \cdot (\mathbf{S}_i \times \mathbf{S}_{i+2})$ (a non-zero z -component of the chirality does not break any continuous symmetry of the model in a field applied along the z -axis and is therefore allowed), reminiscent of the helical order in LiCuVO_4 .

More precisely, DMRG and exact diagonalization have probed signs of long-range chirality correlations [31–33], and the bosonization of the field theory—which unveils a Luttinger liquid phase—predicts $\langle \chi_{i,i+1} \cdot \hat{\mathbf{z}} \rangle \neq 0$ and $\langle \chi_{i,i+2} \cdot \hat{\mathbf{z}} \rangle \neq 0$ [32–34]. The higher-field phase of the model numerically shows evidence of (bond) quadrupolar correlations [2, 3, 32, 33].

Again, here we claim not to provide a detailed description of the material, but we propose that RIXS might be able to probe vector chirality as well as bond-nematic order in this system.

In order to compute the RIXS signal, we proceed like in Ref. 32 closely follow their derivation, and start from the limit $J_1 \ll J_2$ of two decoupled chains (each with lattice spacing $2a_0$). Each one may then be independently bosonized. We use the conventional notations for the boson fields, $\theta_{1,2}$ and $\phi_{1,2}$, where the indices are chain labels, and $[\phi_\nu(x', \tau'), \partial_x \theta_\mu(x, \tau)] = i\delta_{\mu\nu} \delta(x - x') \delta(\tau - \tau')$, for $\mu, \nu = 1, 2$. The spin operators are given by [3, 31, 32, 34]

$$S_\mu^+(x) = e^{i\sqrt{\pi}\theta_\mu(x)} \quad (12)$$

$$\times \left((-1)^j b + b' \sin(2\pi M j + \sqrt{4\pi}\phi_\mu(x)) \right)$$

$$S_\mu^z(x) = M + \frac{1}{\sqrt{\pi}} \partial_x \phi_\mu(x) \quad (13)$$

$$- (-1)^j a \sin(2\pi M j + \sqrt{4\pi}\phi_\mu(x)),$$

where x is the coordinate of a site, while $j \in \mathbb{Z}$ labels a “unit cell” of two sites $\{1, 2\}$ (sites can be labelled by $l = 2j + \mu$), M is the total magnetization (due to the field), and a, b, b' are non-universal constants. Note that here the subscript μ in S_μ^α is unrelated to the subscript i in Eq. (11). As mentioned above, when $J_1 = 0$, the two chains are decoupled and each one obtains two free-boson theories, with the action $\mathcal{S}_{\text{eff}}^\mu = \int dx \int d\tau \left[\frac{v}{2} (K(\partial_x \theta_\mu)^2 + \frac{1}{K}(\partial_x \phi_\mu)^2) + i\partial_x \theta_\mu \partial_\tau \phi_\mu \right]$, where K and v are the Luttinger liquid parameter and spin velocity of the antiferromagnetic Heisenberg (J_2) spin chain in a field. $J_1 \neq 0$ introduces couplings between the chains. Then it is useful to define $\gamma_\pm = (\gamma_1 \pm \gamma_2)/\sqrt{2}$ for $\gamma = \theta, \phi$. The coupling actions are $\mathcal{S}_1 = g_1 \int dx \sin(\sqrt{8\pi}\phi_- + \pi M)$ and $\mathcal{S}_2 = g_2 \int dx (\partial_x \theta_+) \sin \sqrt{2\pi}\theta_-$, where $0 \leq M \leq 1/2$ is the magnetization per site, with parameters $g_1 = -J_1 a^2 \sin \pi M$ and $g_2 = -J_1 \sqrt{\pi} b^2 / \sqrt{2}$, which will lead to “bond nematic” and “vector chiral” phases. This model displays scale invariance, and renormalization group (RG) ideas apply. Then, within this approach, if g_2/g_1 flows to zero (resp. infinity) under the RG flow where high-frequency modes are integrated out, the system goes into the nematic, where ϕ_- gets pinned to a value which minimizes the integrand of \mathcal{S}_1 , (resp. vector chiral, where it is the integrand of \mathcal{S}_2 which acquires a finite expectation value) phase [32]. Details are given in Appendix F 2.

Because each site on the chain has only two neighbors, we expect that the contributions to the RIXS signal from three-spin interactions should be extremely weak. So,

from Table I, assuming a weak enough effect of spin-orbit coupling at the low-energy level, the RIXS transition operator is given by Eq. (7) in zero field, and by

$$T_i = \alpha_{0,\perp} (\boldsymbol{\varepsilon}'^* \cdot \boldsymbol{\varepsilon}_\perp) \mathbf{S}_i^\perp \cdot (\mathbf{S}_{i-1}^\perp + \mathbf{S}_{i+1}^\perp) \quad (14)$$

$$+ \alpha_{0,z} (\boldsymbol{\varepsilon}'^* \cdot \boldsymbol{\varepsilon}_z) S_i^z (S_{i-1}^z + S_{i+1}^z)$$

$$+ (\boldsymbol{\varepsilon}'^* \times \boldsymbol{\varepsilon})^z (\alpha_{1,1,z} \mathbf{S}_i + \alpha_{1,2,z} \mathbf{S}_i \times (\mathbf{S}_{i-1} + \mathbf{S}_{i+1}))^z$$

$$+ \alpha_{2,\perp} [[\boldsymbol{\varepsilon}'^*, \boldsymbol{\varepsilon}]^\perp]^\perp [[\mathbf{S}_i, \mathbf{S}_{i-1} + \mathbf{S}_{i+1}]]^\perp,$$

for $h \neq 0$, i.e. when the full $SU(2)$ symmetry in spin space is broken down to $U(1)$ (see Appendix D). In Eq. (14), we used the definitions $\mathbf{u} = \mathbf{u}_\perp + u^z \hat{\mathbf{z}}$ and $[[\mathbf{u}, \mathbf{v}]]_{\mu\nu}^\perp = \frac{1}{2}(u^\mu v^\nu + v^\nu u^\mu) - \frac{1}{2}(\mathbf{u}_\perp \cdot \mathbf{v}_\perp) \delta_{\mu\nu}$ with $\mu, \nu = x, y$ only. The $\alpha_{n,\mu}$ and $\alpha_{n,m,\mu}$ are coefficients. Finally, we find the following *low-energy* (long distance and time) *leading* contributions (see Appendix F 2) to the RIXS structure factor:

$$\mathcal{I}_{\omega,q}^{\text{nematic}} \propto \sum_{\epsilon=\pm 1} \frac{\Theta(\omega^2 - v_+^2(q - \epsilon\pi)^2)}{\sqrt{\omega^2 - v_+^2(q - \epsilon\pi)^2}^{2-1/K_+}}, \quad (15)$$

for, e.g., $\boldsymbol{\varepsilon} \times \boldsymbol{\varepsilon}'^* = \mathbf{0}$ and $\boldsymbol{\varepsilon} \perp \hat{\mathbf{z}}$ in the nematic phase, and, around $q = \pm 2\pi M \pm \pi$:

$$\mathcal{I}_{\omega,q}^{\text{chiral}} \propto \sum_{\epsilon, \epsilon'=\pm 1} \Theta(\omega^2 - v_+^2(q - 2\pi\epsilon M - \epsilon'\pi)^2) \quad (16)$$

$$\times \sqrt{\omega^2 - v_+^2(q - 2\pi\epsilon M - \epsilon'\pi)^2}^{4K_+ - 2}$$

in cross polarizations, with $(\boldsymbol{\varepsilon} \times \boldsymbol{\varepsilon}'^*) \parallel \hat{\mathbf{z}}$ in the vector chiral phase. In the expressions above, $K_+ = K(1 + J_1 \frac{K}{\pi v})$ and $v_+ = v(1 - J_1 \frac{K}{\pi v})$ [note that $K(M=0) = 1/2$ and $K(M=1/2) = 1$]. Figure 2 displays some examples.

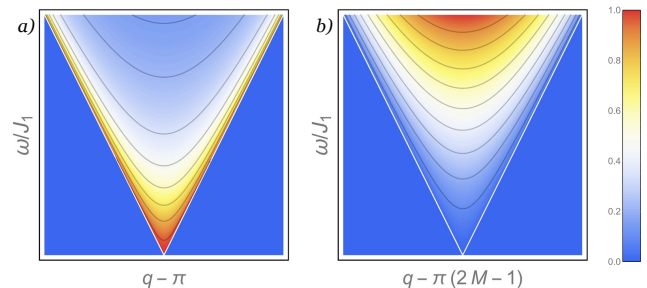


FIG. 2. Color plots of the dominant contributions to the a) $[[\boldsymbol{\varepsilon}'^*, \boldsymbol{\varepsilon}]^\perp]$ channel (fourth line of Eq. (14)) in the nematic phase, around $q = \pi$, as given in Eq. (15) b) $(\boldsymbol{\varepsilon}'^* \times \boldsymbol{\varepsilon})^z$ channel (third line of Eq. (14)) in the vector-chiral phase, around $q = \pi(2M - 1)$, as given in Eq. (16).

V. OTHER DEGREES OF FREEDOM: ELECTRONS, PHONONS AND ORBITALS

The derivation of effective RIXS operators presented above in the context of magnetic models readily extends

to systems where other degrees of freedom are important. Indeed, the symmetry arguments we employed are general enough that they carry over to any type of problem.

Modifications arise at the level of the identification and choice of basis for the space of operators which act on the local low-energy manifold. In magnetic insulators, as discussed earlier, the natural degrees of freedom are on-site, and a Hamiltonian is always associated with the specification of what the local degrees of freedom, namely effective “spins,” are. More microscopically, one can see an effective spin degree of freedom “emerge” from the multiplet structure of a single-ion Hamiltonian at each site. Now, similarly, if orbital degrees of freedom are to be treated explicitly in an insulating system in RIXS, one may simply introduce a set of (effective) operators \mathbf{L} , $L^\mu L^\nu$ etc., which transform as pseudo-vectors under *real space* operations, and obtain a table similar to Table I, where now each row should be associated with an irreducible representation of the appropriate point group.

Now, systems with charge degrees of freedom, or phonons, are usually approached from a more field-theoretic perspective, where one has lost sight of a microscopic model, and operators are labeled by some momentum index (among others). That being said, given a material, one may always, much like for the insulating magnet case, think about how many electrons, and which single-ion orbital (or spin-orbital), a given ion will “contribute/provide” to the valence band of the whole solid. Provided one can determine this, it is reasonable to think of these spin-orbital states and number of electrons as the building blocks for the local low-energy manifold relevant to RIXS, and the basis of operators can be made of those which reshuffle the electrons in the (single-electron) spin-orbital states (even if the electrons interact, such a non-eigenstate basis can be chosen nevertheless). As an example, consider an atom A contributes n on-site states to the valence band(s) of the system, with creation and annihilation operators $\psi_{\mathbf{r}\alpha}^\dagger, \psi_{\mathbf{r}\alpha}$. One may build on-site operators $\psi_{\mathbf{r}\alpha}^\dagger M_{\alpha\beta} \psi_{\mathbf{r}\beta}$, $\psi_{\mathbf{r}\alpha}^\dagger \psi_{\mathbf{r}\beta}^\dagger M_{\alpha\beta\gamma\delta} \psi_{\mathbf{r}\gamma} \psi_{\mathbf{r}\delta}$ etc., where $\alpha, \beta, \gamma, \delta = 1, \dots, n$ (may be orbital labels, for example), as well as some involving neighbors, $\psi_{\mathbf{r}\alpha}^\dagger M_{\alpha\beta} \psi_{\mathbf{r}'\beta}$, $\psi_{\mathbf{r}\alpha}^\dagger \psi_{\mathbf{r}'\beta}^\dagger M_{\alpha\beta\gamma\delta} \psi_{\mathbf{r}'\gamma} \psi_{\mathbf{r}\delta}$, etc.. Despite the more delocalized nature of the electrons in an itinerant system, a quick order of magnitude estimate shows that, even in a typical metal, only close-neighbor operators are involved in the RIXS transition operators (see Sec. II and footnote therein). An additional constraint in RIXS is charge conservation, since no electrons are kicked out of the sample. Then, much like in the case of magnetic insulators, we may split the tensors M into irreducible representations and obtain the coupling terms to the corresponding combinations of polarizations. In a single band model, for example, the only on-site operators are the density $\psi_{\mathbf{r}}^\dagger \psi_{\mathbf{r}}$ and spin $\psi_{\mathbf{r}}^\dagger \boldsymbol{\sigma} \psi_{\mathbf{r}}$ [35] (and powers thereof, though the latter should be expected to contribute sub-dominantly).

Like in any endeavor to compare experiment with theory, in any other technique, the most-delicate step in the

calculation of a structure factor in a given ground state will be to understand how the $\psi_{\mathbf{r}\alpha}$ operators from the basis act on this ground state and are related to quasiparticle operators, if any. This is particularly true in the case of metals (but also of course in that of, e.g., quantum spin liquids), where, even in the case of a Fermi liquid, where the notion of quasiparticles is meaningful, the quasiparticle operators Ψ^\dagger are, in the crudest approximation, related to the electron operators through the square-root of the quasiparticle weight $0 < Z \leq 1$: $\Psi^\dagger \sim \sqrt{Z} \psi^\dagger$. Therefore, a factor of at least Z^2 will be involved in the contribution of a quasiparticle-related excitation to the RIXS cross-section. Because Z can be very small, like in a highly correlated metal, it is important to keep track of those factors to estimate the (esp. relative) amplitude of a signal of a given origin. For example, upon taking the a *minima* point of view of a single-band Fermi liquid [36] for the overdoped cuprates, one should keep in mind that factors of Z are likely to greatly suppress the quasiparticle contribution to the RIXS signal. This should be crucial in deciphering the origin of the features seen in RIXS spectra of those materials [37–40].

The case of phonons is quite similar. At the symmetry level, phonons bear no spin degree of freedom, but are associated to lattice degrees of freedom and their symmetries. There may be several phonon/displacement modes at each site, so that one can introduce several phonon creation operators $c_{\mathbf{r},a}^\dagger$. The symmetries to be considered should be purely spatial, and related to point group symmetries at site \mathbf{r} . Phonons and orbital degrees of freedom are likely to be important in the context of the nematic order seen in the pnictide superconductors, whose microscopic origin is not yet understood.

Of course, ultimately, the full signal is given by the contributions from all the relevant degrees of freedom.

VI. OUTLOOK

As the above examples have shown, the method presented here is very powerful both in scope and predictive potential. We have, for example, explicitly shown that various hidden orders could be unambiguously identified. Moreover, as we tried to emphasize, this approach offers the advantage of possibly helping with unbiased data analysis since all possible contributions to the RIXS signal can in principle be systematically enumerated.

With this theory in hand, where should one look next? As proposed here, NiGa₂S₄ of course appears as a natural material to investigate with RIXS or REXS. In particular, thanks to $S = 1$ on Ni²⁺ one expects “direct RIXS” processes to be involved and therefore a strong signal. The current resolution on RIXS instruments —of about 130 meV— is too low to detect a sizable signal-to-noise ratio for a material where the exchange has been estimated to lie at around $J \sim 7$ meV (as boldly estimated from a Curie-Weiss temperature of $|\Theta_{\text{CW}}| \sim 80$ K [18]). However, since static order is expected (at higher tem-

peratures) [22], Bragg peaks should appear in REXS (see Fig. 1d)). Spin chain materials like LiCuVO_4 and others [30], while perhaps even more promising in terms of confidence in the realization of a nematic state, will have to await the next generation of RIXS instruments, as their exchange energies are also relatively low (~ 30 K). Perhaps, at this point, high-quality data (like in the cuprates and iridates) would be worth re-investigating in light of all the possibilities which our work unearthed. One can, for example, imagine looking for signs of some of the “stranger” correlation functions presented in Table I. Another exciting direction, briefly mentioned in Section V, is that of pnictide materials, as RIXS may help contribute to the effort of pinning down the origin of the observed nematic order. Finally, most electrifying would perhaps be the detection of chiral order in putative spin liquids on the kagomé lattice [41–43] or the possible appearance of spin quadrupolar correlations (in the absence of dipolar ones) in $\text{La}_{2-x}\text{Ba}_x\text{Cu}_2\text{O}_4$, should it display features of a spin density wave glass [44].

With RIXS taking the central stage in various classes of systems, and new resolution-improved machines on the horizon, the future seems bright for refining our under-

standing of and discovering yet new physics in complex materials amenable to RIXS. And with these general results and derivation in this broad setting, we hope to guide experiments as well as theory in this endeavor. It is also our hope to have somewhat demystified the understanding of RIXS for non-experts of microscopic calculations.

ACKNOWLEDGMENTS

L.S. would like to thank Peter Armitage, Collin Broholm, Radu Coldea, Natalia Drichko, David Hawthorn, Bob Leheny, Kemp Plumb, Daniel Reich and especially Leon Balents for useful discussions. L.S. was generously supported by the Gordon and Betty Moore Foundation through a postdoctoral fellowship of the EPiQS initiative, Grant No. GBMF4303. T.S. was supported by NSF Grant DMR-1305741. This work was also partially supported by a Simons Investigator award from the Simons Foundation to Senthil Todadri.

-
- [1] K. Penc and A. M. Läuchli, *Introduction to Frustrated Magnetism*, edited by C. Lacroix, P. Mendels, and F. Mila, Springer Series in Solid-State Sciences, Vol. 164 (Springer Berlin Heidelberg, 2011) pp. 331–362.
- [2] A. V. Chubukov, “Chiral, nematic, and dimer states in quantum spin chains,” *Phys. Rev. B* **44**, 4693–4696 (1991).
- [3] O. A. Starykh and L. Balents, “Excitations and quasi-one-dimensionality in field-induced nematic and spin density wave states,” *Phys. Rev. B* **89**, 104407 (2014).
- [4] A. Messiah, *Quantum Mechanics* (1962).
- [5] L. J. P. Ament, M. van Veenendaal, T. P. Devereaux, J. P. Hill, and J. van den Brink, “Resonant inelastic x-ray scattering studies of elementary excitations,” *Rev. Mod. Phys.* **83**, 705–767 (2011).
- [6] R. D. Dewey, R. S. Mapes, and T. W. Reynolds, *Handbook of X-ray and microprobe data: Tables of X-ray data*, edited by Elion and Stewart (Oxford, Pergamon Press, 1969).
- [7] J. A. Bearden, “X-ray wavelengths,” *Rev. Mod. Phys.* **39**, 78–124 (1967).
- [8] W.-H. Ko and P. A. Lee, “Proposal for detecting spin-chirality terms in Mott insulators via resonant inelastic x-ray scattering,” *Phys. Rev. B* **84**, 125102 (2011).
- [9] F. Michaud, F. Vernay, and F. Mila, “Theory of inelastic light scattering in spin-1 systems: Resonant regimes and detection of quadrupolar order,” *Phys. Rev. B* **84**, 184424 (2011).
- [10] M. W. Haverkort, “Theory of resonant inelastic x-ray scattering by collective magnetic excitations,” *Phys. Rev. Lett.* **105**, 167404 (2010).
- [11] The “diamagnetic” term \mathbf{A}^2 , of second order in \mathbf{A} , is involved in the *first-order* contribution to the scattering amplitude, which is negligible close to resonance.
- [12] For $\omega^{\text{x-ray}} \sim 10$ keV, $|\mathbf{k}| \sim 1 \text{ \AA}^{-1}$ and $|\mathbf{k} \cdot \delta\mathbf{r}| \approx 0$ can seem hardly valid. In practice, however it has been shown to usually be a good approximation. Regardless, we discuss how to go beyond this approximation in Appendix E.
- [13] Indeed, $\tau \sim 10^{-15}$ s corresponds to an energy of order 4 eV, which is typically that of a metal’s bandwidth W . Taking estimate of an electron’s velocity as $v = aW$ with a the lattice spacing, we find that the travelled distance during time τ of order a lattice spacing.
- [14] M. W. Haverkort, N. Hollmann, I. P. Krug, and A. Tanaka, “Symmetry analysis of magneto-optical effects: The case of x-ray diffraction and x-ray absorption at the transition metal $L_{2,3}$ edge,” *Phys. Rev. B* **82**, 094403 (2010).
- [15] More rigorously, one should derive the transition operators in terms of spin-orbit coupled effective spins, and *then* possibly neglect those which are not rotationally symmetric.
- [16] D. W. Snoke, “Point groups,” .
- [17] Note that Ref. 10 additionally provides a relation between some of the coefficients α_β and absorption spectroscopy coefficients.
- [18] S. Nakatsuji, Y. Nambu, H. Tonomura, O. Sakai, S. Jonas, C. Broholm, H. Tsunetsugu, Y. Qiu, and Y. Maeno, “Spin disorder on a triangular lattice,” *Science* **309**, 1697–1700 (2005), <http://www.sciencemag.org/content/309/5741/1697.full.pdf>.
- [19] H. Tsunetsugu and M. Arikawa, “Spin nematic phase in $S = 1$ triangular antiferromagnets,” *J. Phys. Soc. Jpn* **75**, 083701 (2006), <http://dx.doi.org/10.1143/JPSJ.75.083701>.
- [20] A. Läuchli, F. Mila, and K. Penc, “Quadrupolar phases of the $S = 1$ bilinear-biquadratic Heisenberg model on the triangular lattice,” *Phys. Rev. Lett.* **97**, 087205

- (2006).
- [21] S. Bhattacharjee, V. B. Shenoy, and T. Senthil, “Possible ferro-spin nematic order in NiGa_2S_4 ,” *Phys. Rev. B* **74**, 092406 (2006).
- [22] E. M. Stoudenmire, S. Trebst, and L. Balents, “Quadrupolar correlations and spin freezing in $S = 1$ triangular lattice antiferromagnets,” *Phys. Rev. B* **79**, 214436 (2009).
- [23] R. Kaul, “Spin nematic ground state of the triangular lattice $S = 1$ biquadratic model,” *Phys. Rev. B* **86**, 104411 (2012).
- [24] A. Smerald and N. Shannon, “Theory of spin excitations in a quantum spin-nematic state,” *Phys. Rev. B* **88**, 184430 (2013).
- [25] A. S. T. Pires, “Dynamics of the ferroquadrupolar phase of the $S = 1$ bilinear-biquadratic model on the triangular lattice,” *Solid State Communications* **196**, 24–27 (2014).
- [26] A. Völl and S. Wessel, “Spin dynamics of the bilinear-biquadratic $S = 1$ Heisenberg model on the triangular lattice: A quantum Monte Carlo study,” *Phys. Rev. B* **91**, 165128 (2015).
- [27] M. Enderle, C. Mukherjee, B. Fåk, R. K. Kremer, J.-M. Broto, H. Rosner, S.-L. Drechsler, J. Richter, J. Malek, A. Prokofiev, W. Assmus, S. Pujol, J.-L. Raggazzoni, H. Rakoto, M. Rheinstädter, and H. M. Rønnow, “Quantum helimagnetism of the frustrated spin-1/2 chain LiCuVO_4 ,” *EPL (Europhysics Letters)* **70**, 237 (2005).
- [28] M. Hagiwara, L. E. Svistov, T. Fujita, H. Yamaguchi, S. Kimura, K. Omura, A. Prokofiev, A. I. Smirnov, and Z. Honda, “Possibility of the field-induced spin-nematic phase in LiCuVO_4 ,” *Journal of Physics: Conference Series* **320**, 012049 (2011).
- [29] M. Mourigal, M. Enderle, B. Fåk, R. Kremer, J. Law, A. Schneidewind, A. Hiess, and A. Prokofiev, “Evidence of a bond-nematic phase in licuvo_4 ,” *Phys. Rev. Lett.* **109**, 027203 (2012).
- [30] K. Nawa, Y. Okamoto, A. Matsuo, K. Kindo, Y. Kitahara, S.a Yoshida, S. Ikeda, S. Hara, T. Sakurai, S. Okubo, H. Ohta, and Z. Hiroi, “ $\text{NaCuMoO}_4(\text{OH})$ as a candidate frustrated $J_1 - J_2$ chain quantum magnet,” *Journal of the Physical Society of Japan* **83**, 103702 (2014).
- [31] A. Kolezhuk and T. Vekua, “Field-induced chiral phase in isotropic frustrated spin chains,” *Phys. Rev. B* **72**, 094424 (2005).
- [32] T. Hikihara, L. Kecke, T. Momoi, and A. Furusaki, “Vector chiral and multipolar orders in the spin- $\frac{1}{2}$ frustrated ferromagnetic chain in magnetic field,” *Phys. Rev. B* **78**, 144404 (2008).
- [33] J. Sudan, A. Lüscher, and A. Läuchli, “Emergent multipolar spin correlations in a fluctuating spiral: The frustrated ferromagnetic spin- $\frac{1}{2}$ Heisenberg chain in a magnetic field,” *Phys. Rev. B* **80**, 140402 (2009).
- [34] I. P. McCulloch, R. Kube, M. Kurz, A. Kleine, U. Schollwöck, and A. K. Kolezhuk, “Vector chiral order in frustrated spin chains,” *Phys. Rev. B* **77**, 094404 (2008).
- [35] P. Marra, S. Sykora, K. Wohlfeld, and J. van den Brink, “Resonant inelastic x-ray scattering as a probe of the phase and excitations of the order parameter of superconductors,” *Phys. Rev. Lett.* **110**, 117005 (2013).
- [36] D. Benjamin, I. Klich, and E. Demler, “Single-band model of resonant inelastic x-ray scattering by quasiparticles in high- T_c cuprate superconductors,” *Phys. Rev. Lett.* **112**, 247002 (2014).
- [37] M. Le Tacon, G. Ghiringhelli, J. Chaloupka, M. Moretti Sala, V. Hinkov, M. W. Haverkort, M. Minola, M. Bakr, K. J. Zhou, S. Blanco-Canosa, C. Monney, Y. T. Song, G. L. Sun, C. T. Lin, G. M. De Luca, M. Salluzzo, G. Khaliullin, T. Schmitt, L. Braicovich, and B. Keimer, “Intense paramagnon excitations in a large family of high-temperature superconductors,” *Nat. Phys.* **7**, 725–730 (2011).
- [38] M. Le Tacon, M. Minola, D. C. Peets, M. Moretti Sala, S. Blanco-Canosa, V. Hinkov, R. Liang, D. A. Bonn, W. N. Hardy, C. T. Lin, T. Schmitt, L. Braicovich, G. Ghiringhelli, and B. Keimer, “Dispersive spin excitations in highly overdoped cuprates revealed by resonant inelastic x-ray scattering,” *Phys. Rev. B* **88**, 020501 (2013).
- [39] M. P. M. Dean, G. Dellea, R. S. Springell, F. Yakhov-Harris, K. Kummer, N. B. Brookes, X. Liu, Y.-J. Sun, J. Strle, T. Schmitt, L. Braicovich, G. Ghiringhelli, I. Bozovic, and J. P. Hill, “Persistence of magnetic excitations in $\text{La}_{2-x}\text{Sr}_x\text{CuO}_4$ from the undoped insulator to the heavily overdoped non-superconducting metal,” *Nat. Mater.* **12**, 1019–1023 (2013).
- [40] S. Wakimoto, K. Ishii, H. Kimura, M. Fujita, G. Dellea, K. Kummer, L. Braicovich, G. Ghiringhelli, L. M. Debeer-Schmitt, and G. E. Granroth, “High-energy magnetic excitations in overdoped $\text{La}_{2x}\text{Sr}_x\text{CuO}_4$ studied by neutron and resonant inelastic x-ray scattering,” *arXiv:1505.03945* (2015).
- [41] W.-J. Hu, W. Zhu, Y. Zhang, S. Gong, F. Becca, and D. N. Sheng, “Variational monte carlo study of a chiral spin liquid in the extended Heisenberg model on the kagome lattice,” *Phys. Rev. B* **91**, 041124 (2015).
- [42] S.-S. Gong, W. Zhu, L. Balents, and D. N. Sheng, “Global phase diagram of competing ordered and quantum spin-liquid phases on the kagome lattice,” *Phys. Rev. B* **91**, 075112 (2015).
- [43] A. Wietek, A. Sterdyniak, and A. M. Läuchli, “Nature of chiral spin liquids on the kagome lattice,” (2015), *arXiv:1503.03389*.
- [44] D. F. Mross and T. Senthil, “Spin and pair density wave glasses,” (2015), *arXiv:1502.00002*.
- [45] One may also write the R transformation as $S^\mu \rightarrow U_R^\dagger S^\mu U_R$, where U_R acts in spin space (U_R is the operator that R maps into through the appropriate representation of the symmetry group).
- [46] Dorothy G. Bell, “Group theory and crystal lattices,” *Rev. Mod. Phys.* **26**, 311–320 (1954).
- [47] G. F. Koster, J. O. Dimmock, R. G. Wheeler, and H. Statz, *Properties of the Thirty-Two Point Groups* (MIT Press, Cambridge, 1963).
- [48] J. Goss, “Point group symmetry,” .

Appendix A: Electromagnetic field

As mentioned in the main text, the electromagnetic vector potential at point \mathbf{r} may be expanded in plane waves

$$\mathbf{A}(\mathbf{r}) = \sum_{\mathbf{k}} \sqrt{\frac{\hbar}{2V\epsilon_0\omega_{\mathbf{k}}}} \sum_{\epsilon} \left(\epsilon^* a_{\mathbf{k},\epsilon}^\dagger e^{-i\mathbf{k}\cdot\mathbf{r}} + \text{h.c.} \right), \quad (\text{A1})$$

where \hbar is Planck's constant, ϵ_0 is the vacuum dielectric polarization, $\omega_{\mathbf{k}} = \omega_{-\mathbf{k}} = c|\mathbf{k}|$, with c the speed of light, V is the volume in which the electromagnetic field is confined, $\boldsymbol{\varepsilon}$ has nonzero components only along (real) vectors perpendicular to \mathbf{k} , and we define $\mathbf{A}_{\mathbf{k},\boldsymbol{\varepsilon}}(\mathbf{r}) = \boldsymbol{\varepsilon}^* a_{\mathbf{k},\boldsymbol{\varepsilon}}^\dagger e^{-i\mathbf{k}\cdot\mathbf{r}} + \text{h.c.}$. $a_{\mathbf{k},\boldsymbol{\varepsilon}}^\dagger$ is the creation operator of a photon of momentum \mathbf{k} and polarization (helicity) $\boldsymbol{\varepsilon}$. This ‘‘expansion’’ introduces (and defines) the polarization vector $\boldsymbol{\varepsilon}$ which encodes the vectorial (in the sense of a tensor of rank one) nature of the $S = 1$ field \mathbf{A} . We return to the symmetry transformation rules of \mathbf{A} and $\boldsymbol{\varepsilon}$ in Appendix B.

Appendix B: Transformation rules

The (pseudo-)vector of spin operators $\mathbf{S}_{\mathbf{r}}$ transforms under a spatial operation R and time reversal (TR) according to

$$\begin{cases} R: & \mathbf{S}_{\mathbf{r}} \rightarrow \det(R)R \cdot \mathbf{S}_{R\cdot\mathbf{r}} \\ \text{TR}: & \mathbf{S}_{\mathbf{r}} \rightarrow -\mathbf{S}_{\mathbf{r}} \end{cases}, \quad (\text{B1})$$

regardless of the value of $S(S+1)$ [45]. The vector potential \mathbf{A} transforms as

$$\begin{cases} R: & \mathbf{A}(\mathbf{r}) \rightarrow R \cdot \mathbf{A}(R \cdot \mathbf{r}) \\ \text{TR}: & \mathbf{A}(\mathbf{r}) \rightarrow -\mathbf{A}(\mathbf{r}) \end{cases}, \quad (\text{B2})$$

so that the polarization $\boldsymbol{\varepsilon}$ transforms according to

$$\begin{cases} R: & \boldsymbol{\varepsilon} \rightarrow R \cdot \boldsymbol{\varepsilon} \\ \text{TR}: & \boldsymbol{\varepsilon} \rightarrow -\boldsymbol{\varepsilon}^* \end{cases}. \quad (\text{B3})$$

Note that the definition of the polarization sometimes differs by, e.g., a factor of i , and the polarization is then ‘‘even’’ (times complex conjugation) under the time reversal operation.

If the spatial symmetry group contains all spherical operations (which contain in particular all $SO(3)$ operations), \mathbf{S} and $\boldsymbol{\varepsilon}$ transform under the ‘‘ $L = 1$ ’’ representation of $SO(3)$ (regardless of the value of $S(S+1)$). Note that here, the name ‘‘ L ’’ is purely formal. Using the notation from Ref. 16 for the full rotational symmetry group ‘‘ D ’’ ($SO(3) \subset D$), $\boldsymbol{\varepsilon}$ and \mathbf{S} transform under the D_1^- and D_1^+ representations, respectively, where \pm indicate parity under the inversion transformation.

Appendix C: Derivation of Table I

In the equations below, the numbers are representation labels ($L = 0, 1, 2, \dots$ associated to D_L^\pm), and the superscripts *schematically* show basis elements (in the form of tensors) in terms of the original terms in the products. Products of representations for

- zero spins:

$$1^{\boldsymbol{\varepsilon}'} \times 1^\boldsymbol{\varepsilon} = \left(0^{\boldsymbol{\varepsilon}' \cdot \boldsymbol{\varepsilon}} + 1^{\boldsymbol{\varepsilon}' \times \boldsymbol{\varepsilon}} + 2^{\llbracket \boldsymbol{\varepsilon}', \boldsymbol{\varepsilon} \rrbracket} \right); \quad (\text{C1})$$

- one spin:

$$1^{\boldsymbol{\varepsilon}'} \times 1^\boldsymbol{\varepsilon} \times 1^{\mathbf{S}_i} = \left(0^{\boldsymbol{\varepsilon}' \cdot \boldsymbol{\varepsilon}} + 1^{\boldsymbol{\varepsilon}' \times \boldsymbol{\varepsilon}} + 2^{\llbracket \boldsymbol{\varepsilon}', \boldsymbol{\varepsilon} \rrbracket} \right) \times 1^{\mathbf{S}_i}; \quad (\text{C2})$$

- two spins:

$$1^{\boldsymbol{\varepsilon}'} \times 1^\boldsymbol{\varepsilon} \times 1^{\mathbf{S}_i} \times 1^{\mathbf{S}_j} = \left(0^{\boldsymbol{\varepsilon}' \cdot \boldsymbol{\varepsilon}} + 1^{\boldsymbol{\varepsilon}' \times \boldsymbol{\varepsilon}} + 2^{\llbracket \boldsymbol{\varepsilon}', \boldsymbol{\varepsilon} \rrbracket} \right) \times \left(0^{\mathbf{S}_i \cdot \mathbf{S}_j} + 1^{\mathbf{S}_i \times \mathbf{S}_j} + 2^{\llbracket \mathbf{S}_i, \mathbf{S}_j \rrbracket} \right); \quad (\text{C3})$$

- three spins:

$$\begin{aligned} & 1^{\boldsymbol{\varepsilon}'} \times 1^\boldsymbol{\varepsilon} \times 1^{\mathbf{S}_i} \times 1^{\mathbf{S}_j} \times 1^{\mathbf{S}_k} \quad (\text{C4}) \\ &= \left(0^{\boldsymbol{\varepsilon}' \cdot \boldsymbol{\varepsilon}} + 1^{\boldsymbol{\varepsilon}' \times \boldsymbol{\varepsilon}} + 2^{\llbracket \boldsymbol{\varepsilon}', \boldsymbol{\varepsilon} \rrbracket} \right) \\ & \quad \times \left(0^{\mathbf{S}_i \cdot \mathbf{S}_j} + 1^{\mathbf{S}_i \times \mathbf{S}_j} + 2^{\llbracket \mathbf{S}_i, \mathbf{S}_j \rrbracket} \right) \times 1^{\mathbf{S}_k} \\ &= \left(0^{\boldsymbol{\varepsilon}' \cdot \boldsymbol{\varepsilon}} + 1^{\boldsymbol{\varepsilon}' \times \boldsymbol{\varepsilon}} + 2^{\llbracket \boldsymbol{\varepsilon}', \boldsymbol{\varepsilon} \rrbracket} \right) \\ & \quad \times \left(1^{(\mathbf{S}_i \cdot \mathbf{S}_j)\mathbf{S}_k} + 0^{(\mathbf{S}_i \times \mathbf{S}_j) \cdot \mathbf{S}_k} + 1^{(\mathbf{S}_i \times \mathbf{S}_j) \times \mathbf{S}_k} \right. \\ & \quad \left. + 2^{\llbracket (\mathbf{S}_i \times \mathbf{S}_j), \mathbf{S}_k \rrbracket} + 1^{\llbracket \mathbf{S}_i, \mathbf{S}_j \rrbracket \cdot \mathbf{S}_k} + 2^{\llbracket \mathbf{S}_i, \mathbf{S}_j \rrbracket \times \mathbf{S}_k} \right. \\ & \quad \left. + 3^{\llbracket \llbracket \mathbf{S}_i, \mathbf{S}_j \rrbracket, \mathbf{S}_k \rrbracket} \right), \end{aligned}$$

where the definition of the double brackets has been extended to:

$$\begin{cases} (\llbracket \mathbf{u}, \mathbf{v} \rrbracket \cdot \mathbf{w})_\mu = \sum_\nu \llbracket \mathbf{u}, \mathbf{v} \rrbracket_{\mu\nu} w_\nu \\ (\llbracket \mathbf{u}, \mathbf{v} \rrbracket \times \mathbf{w})_{\mu\rho} = \sum_{\nu,\lambda} \epsilon_{\nu\lambda\rho} \llbracket \mathbf{u}, \mathbf{v} \rrbracket_{\mu\nu} w_\lambda \\ (\llbracket \llbracket \mathbf{u}, \mathbf{v} \rrbracket, \mathbf{w} \rrbracket)_{\mu\nu\lambda} = \llbracket \mathbf{u}, \mathbf{v} \rrbracket_{\mu\nu} w_\lambda \end{cases} \quad (\text{C5})$$

Only products of terms belonging to the same representation will have a contribution in the ‘‘final’’ 0 representation (by contracting all the indices).

Explicitly, the operator obtained for all the terms in Table I reads:

$$\begin{aligned} T &= (\boldsymbol{\varepsilon}'^* \cdot \boldsymbol{\varepsilon}) [a_{0,1} \mathbf{S}_i \cdot \mathbf{S}_j + a_{0,2} (\mathbf{S}_i \times \mathbf{S}_j) \cdot \mathbf{S}_k] \quad (\text{C6}) \\ &+ (\boldsymbol{\varepsilon}'^* \times \boldsymbol{\varepsilon}) \cdot [a_{1,1} \mathbf{S}_i + a_{1,2} \mathbf{S}_i \times \mathbf{S}_j + a_{1,3} (\mathbf{S}_i \cdot \mathbf{S}_j) \mathbf{S}_k \\ & \quad + a_{1,4} (\mathbf{S}_i \times \mathbf{S}_j) \times \mathbf{S}_k + a_{1,5} \llbracket \mathbf{S}_i, \mathbf{S}_j \rrbracket \cdot \mathbf{S}_k] \\ &+ \llbracket \boldsymbol{\varepsilon}'^*, \boldsymbol{\varepsilon} \rrbracket (a_{2,1} \llbracket \mathbf{S}_i, \mathbf{S}_j \rrbracket + a_{2,2} \llbracket \mathbf{S}_i \times \mathbf{S}_j, \mathbf{S}_k \rrbracket \\ & \quad + a_{2,3} \llbracket \mathbf{S}_i, \mathbf{S}_j \rrbracket \times \mathbf{S}_k). \end{aligned}$$

Appendix D: Lower symmetry

It has been pointed out [14] that, even when spin-orbit coupling is negligible in the low-energy manifold, spin-orbit is always very strong in core levels, and may lead

to anisotropies in the RIXS signal. The derivation provided in the main text is readily generalized to the case of discrete “spin” symmetries.

With the help of the tables found in Refs. 16, 46–48, one may build bases for the representations, generalizing those of rotationally-invariant systems. The formula which generalizes Eq. (C6) is:

$$T_{\mathbf{R}} = \sum_{\Gamma} \sum_l \alpha_{\Gamma,l} \mathcal{E}^{\Gamma,l} \cdot \mathcal{S}^{\Gamma,l}, \quad (\text{D1})$$

where the sum proceeds over all irreducible representations Γ of the point symmetry group at site \mathbf{R} (that of the core hole), l indexes the multiplicity of the representation Γ , and the dot product represents a symmetric contraction of all indices.

Appendix E: Higher multipoles

As mentioned in the main text, the Hamiltonian at first order in \mathbf{A} is actually

$$H' = \sum_{\mathbf{r}} \left[\hat{\psi}_{\mathbf{r}}^{\dagger} \frac{e\mathbf{p}}{m} \hat{\psi}_{\mathbf{r}} \cdot \mathbf{A} + \hat{\psi}_{\mathbf{r}}^{\dagger} \frac{e\hbar\boldsymbol{\sigma}}{2m} \hat{\psi}_{\mathbf{r}} \cdot (\nabla \times \mathbf{A}_{\mathbf{r}}) \right]. \quad (\text{E1})$$

In the main text, only the first term was considered. In the spirit of the derivation provided in the main text, where experimental parameters are kept explicit, to treat the second term, one should consider the couplings to $\mathbf{k} \times \boldsymbol{\varepsilon}$ and $\mathbf{k}' \times \boldsymbol{\varepsilon}'$, much as we did to $\boldsymbol{\varepsilon}$ and $\boldsymbol{\varepsilon}'$ upon considering the term linear in \mathbf{p} . One should also note that “higher multipoles” will also arise from the expansion of the exponential, $e^{i\mathbf{k} \cdot \delta\mathbf{r}} = 1 + i\mathbf{k} \cdot \delta\mathbf{r} - \frac{1}{2}(\mathbf{k} \cdot \delta\mathbf{r})^2 + \dots$.

Appendix F: Details of the cross-section derivations

1. Spin nematic in $S = 1$ triangular magnets

Following Ref. 19 (the calculation is performed there in the antiferroquadrupolar phase), we introduce the bosonic operators $\alpha_{\mathbf{r}}$ and $\beta_{\mathbf{r}}$, and the Fock space vacuum such that

$$\begin{cases} |S_{\mathbf{r}}^z = 0\rangle = |\text{vac}\rangle \\ |S_{\mathbf{r}}^z = \pm 1\rangle = \frac{1}{\sqrt{2}}(\alpha_{\mathbf{r}}^{\dagger} \pm i\beta_{\mathbf{r}}^{\dagger})|\text{vac}\rangle \end{cases}, \quad (\text{F1})$$

and

$$\begin{cases} S_{\mathbf{r}}^x = \alpha_{\mathbf{r}}^{\dagger} + \alpha_{\mathbf{r}} \\ S_{\mathbf{r}}^y = \beta_{\mathbf{r}}^{\dagger} + \beta_{\mathbf{r}} \\ S_{\mathbf{r}}^z = -i(\alpha_{\mathbf{r}}^{\dagger}\beta_{\mathbf{r}} - \beta_{\mathbf{r}}^{\dagger}\alpha_{\mathbf{r}}) \end{cases}, \quad (\text{F2})$$

with the constraint that there should be no more than one boson per site. This in particular implies, in real space:

$$\begin{cases} \alpha_{\mathbf{r}}^2 = \beta_{\mathbf{r}}^2 = \alpha_{\mathbf{r}}\beta_{\mathbf{r}} = \beta_{\mathbf{r}}\alpha_{\mathbf{r}} = 0 \\ \alpha_{\mathbf{r}}\beta_{\mathbf{r}}^{\dagger} = \beta_{\mathbf{r}}\alpha_{\mathbf{r}}^{\dagger} = 0 \\ \alpha_{\mathbf{r}}\alpha_{\mathbf{r}}^{\dagger} = \beta_{\mathbf{r}}\beta_{\mathbf{r}}^{\dagger} = 1 - \alpha_{\mathbf{r}}^{\dagger}\alpha_{\mathbf{r}} - \beta_{\mathbf{r}}^{\dagger}\beta_{\mathbf{r}} \end{cases}. \quad (\text{F3})$$

Furthermore,

$$(\mathbf{S}_i \cdot \mathbf{S}_j)^2 = -\frac{1}{2}\mathbf{S}_i \cdot \mathbf{S}_j + \frac{1}{4} \sum_{\mu,\nu} \{S_i^{\mu}, S_i^{\nu}\} \{S_j^{\mu}, S_j^{\nu}\}, \quad (\text{F4})$$

and

$$\begin{aligned} \frac{1}{4} \sum_{\mu,\nu} \{S_i^{\mu}, S_i^{\nu}\} \{S_j^{\mu}, S_j^{\nu}\} \\ = \sum_{\mu} (S_i^{\mu})^2 (S_j^{\mu})^2 + \frac{1}{2} \sum_{\nu > \mu} \{S_i^{\mu}, S_i^{\nu}\} \{S_j^{\mu}, S_j^{\nu}\}, \end{aligned} \quad (\text{F5})$$

with

$$\begin{cases} \{S_{\mathbf{r}}^x, S_{\mathbf{r}}^y\} = \alpha_{\mathbf{r}}^{\dagger}\beta_{\mathbf{r}} + \beta_{\mathbf{r}}^{\dagger}\alpha_{\mathbf{r}} \\ \{S_{\mathbf{r}}^x, S_{\mathbf{r}}^z\} = -i(\beta_{\mathbf{r}} - \beta_{\mathbf{r}}^{\dagger}) \\ \{S_{\mathbf{r}}^y, S_{\mathbf{r}}^z\} = -i(-\alpha_{\mathbf{r}} + \alpha_{\mathbf{r}}^{\dagger}) \\ (S_{\mathbf{r}}^x)^2 = 1 - \beta_{\mathbf{r}}^{\dagger}\beta_{\mathbf{r}} \\ (S_{\mathbf{r}}^y)^2 = 1 - \alpha_{\mathbf{r}}^{\dagger}\alpha_{\mathbf{r}} \\ (S_{\mathbf{r}}^z)^2 = \alpha_{\mathbf{r}}^{\dagger}\alpha_{\mathbf{r}} + \beta_{\mathbf{r}}^{\dagger}\beta_{\mathbf{r}} \end{cases} \quad (\text{F6})$$

Using the rules Eq. (F3) and then keeping only terms quadratic in the boson operators $\alpha_{\mathbf{r}}$, $\alpha_{\mathbf{r}}^{\dagger}$, $\beta_{\mathbf{r}}$ and $\beta_{\mathbf{r}}^{\dagger}$ (i.e. neglecting interactions between the bosons), we arrive at

$$\begin{aligned} H &= \frac{1}{2} (J_1 - J_2) \sum_{\eta=\alpha,\beta} \sum_{\mathbf{r}} \sum_n \left[\eta_{\mathbf{r}}^{\dagger} \eta_{\mathbf{r}+\mathbf{R}_n}^{\dagger} + \eta_{\mathbf{r}} \eta_{\mathbf{r}+\mathbf{R}_n} \right] \\ &+ \frac{J_1}{2} \sum_{\eta=\alpha,\beta} \sum_{\mathbf{r}} \sum_n \left[\eta_{\mathbf{r}}^{\dagger} \eta_{\mathbf{r}+\mathbf{R}_n} + \eta_{\mathbf{r}} \eta_{\mathbf{r}+\mathbf{R}_n}^{\dagger} \right] \\ &- \frac{J_2}{2} \sum_{\eta=\alpha,\beta} \sum_{\mathbf{r}} \sum_n \left[\eta_{\mathbf{r}}^{\dagger} \eta_{\mathbf{r}} + \eta_{\mathbf{r}+\mathbf{R}_n}^{\dagger} \eta_{\mathbf{r}+\mathbf{R}_n} \right] \\ &= \frac{\gamma_{\mathbf{k}}}{2} (J_1 - J_2) \sum_{\eta=\alpha,\beta} \sum_{\mathbf{k}} \left[\eta_{\mathbf{k}}^{\dagger} \eta_{-\mathbf{k}}^{\dagger} + \eta_{\mathbf{k}} \eta_{-\mathbf{k}} \right] \\ &+ (J_1 \gamma_{\mathbf{k}} - 6J_2) \sum_{\eta=\alpha,\beta} \sum_{\mathbf{k}} \eta_{\mathbf{k}}^{\dagger} \eta_{\mathbf{k}}, \end{aligned} \quad (\text{F7})$$

where $\gamma_{\mathbf{k}} = 2(\cos k_x + \cos(\frac{1}{2}(k_x + \sqrt{3}k_y))) + \cos(\frac{1}{2}(k_x - \sqrt{3}k_y))$. With the Bogoliubov transformation $\eta_{\mathbf{k}}^{\dagger} = \cosh \xi_{\mathbf{k}} \rho_{\mathbf{k}}^{\dagger} + \sinh \xi_{\mathbf{k}} \rho_{-\mathbf{k}}$, we obtain

$$H = \sum_{\rho=\rho^{\alpha},\rho^{\beta}} \sum_{\mathbf{k}} \omega_{\mathbf{k}} \rho_{\mathbf{k}}^{\dagger} \rho_{\mathbf{k}}, \quad (\text{F8})$$

where we have defined:

$$\omega_{\mathbf{k}} = 2[A_{\mathbf{k}} \cosh 2\xi_{\mathbf{k}} + B_{\mathbf{k}} \sinh 2\xi_{\mathbf{k}}] = 2\sqrt{A_{\mathbf{k}}^2 - B_{\mathbf{k}}^2}, \quad (\text{F9})$$

with

$$\begin{cases} A_{\mathbf{k}} = \frac{1}{2}(J_1 \gamma_{\mathbf{k}} - 6J_2) \\ B_{\mathbf{k}} = \frac{\gamma_{\mathbf{k}}}{2}(J_2 - J_1) \end{cases} \quad (\text{F10})$$

if

$$\begin{cases} A_{\mathbf{k}} \sinh 2\xi_{\mathbf{k}} + B_{\mathbf{k}} \cosh 2\xi_{\mathbf{k}} = 0 \\ (A_{\mathbf{k}} \cosh 2\xi_{\mathbf{k}} + B_{\mathbf{k}} \sinh 2\xi_{\mathbf{k}})^2 = A_{\mathbf{k}}^2 - B_{\mathbf{k}}^2 \end{cases}. \quad (\text{F11})$$

This yields:

$$\begin{cases} \sinh^2 2\xi_{\mathbf{k}} = \frac{B_{\mathbf{k}}^2}{A_{\mathbf{k}}^2 - B_{\mathbf{k}}^2} \\ \cosh^2 2\xi_{\mathbf{k}} = \frac{A_{\mathbf{k}}^2}{A_{\mathbf{k}}^2 - B_{\mathbf{k}}^2} \end{cases}. \quad (\text{F12})$$

Since $\forall x \cosh x > 0$,

$$\cosh 2\xi_{\mathbf{k}} = \sqrt{\frac{A_{\mathbf{k}}^2}{A_{\mathbf{k}}^2 - B_{\mathbf{k}}^2}}, \quad \sinh 2\xi_{\mathbf{k}} = -\frac{B_{\mathbf{k}}}{A_{\mathbf{k}}} \sqrt{\frac{A_{\mathbf{k}}^2}{A_{\mathbf{k}}^2 - B_{\mathbf{k}}^2}}. \quad (\text{F13})$$

The transition operator Eq. (6) takes the form, in Fourier space:

$$T_{\mathbf{k}} = \kappa^{(0)} \delta(\mathbf{k}) - \sum_{\mu} \sum_{\rho=\rho^{\mu}} \left[\rho_{\mathbf{k}}^{\dagger} (\mathcal{A}_{\mu} \cosh \xi_{\mathbf{k}} + \mathcal{B}_{\mu} \sinh \xi_{\mathbf{k}}) + \rho_{-\mathbf{k}} (\mathcal{A}_{\mu} \sinh \xi_{\mathbf{k}} + \mathcal{B}_{\mu} \cosh \xi_{\mathbf{k}}) \right], \quad (\text{F14})$$

where

$$\kappa^{(0)} = \alpha_0 (\boldsymbol{\varepsilon} \cdot \boldsymbol{\varepsilon}'^*) \quad (\text{F15})$$

$$\kappa_{\mu}^{(1)} = \alpha_1 \epsilon_{\mu\sigma\tau} \varepsilon^{\sigma} \varepsilon'^{* \tau} \quad (\text{F16})$$

$$\kappa_{\mu\nu}^{(2)} = \alpha_2 \left[-\frac{2}{3} \delta_{\mu\nu} (\boldsymbol{\varepsilon} \cdot \boldsymbol{\varepsilon}'^*) + \varepsilon^{\mu} \varepsilon'^{* \nu} + \varepsilon^{\nu} \varepsilon'^{* \mu} \right] \quad (\text{F17})$$

$$\mathcal{A}_x = \kappa_{xy}^{(2)} + i\kappa_z \quad (\text{F18})$$

$$\mathcal{A}_x = \kappa_{yz}^{(2)} - i\kappa_x \quad (\text{F19})$$

$$\mathcal{B}_x = \kappa_{xy}^{(2)} - i\kappa_z \quad (\text{F20})$$

$$\mathcal{B}_x = \kappa_{yz}^{(2)} + i\kappa_x. \quad (\text{F21})$$

Plugging this into the expression for the cross section:

$$\frac{\delta^2 \sigma}{\delta \Omega \delta \omega} \propto \sum_{\mu=x,z} |\mathcal{A}_{\mu} \cosh \xi_{\mathbf{k}} + \mathcal{B}_{\mu} \sinh \xi_{\mathbf{k}}|^2 \delta(\omega - \omega_{\mathbf{k}}),$$

we arrive at the result given in the main text.

2. Vector chirality and bond nematic in $S = 1/2$ $J_1 - J_2$ chains

Equal-time and real-space correlation functions are given in Refs. [32, 34]. Here, we find the following contributions to the cross section:

- in the nematic phase:

$$\mathcal{I}^{((S^+ S^+)_{-\omega, -k} (S^+ S^+)_{\omega, k})} \quad (\text{F22})$$

$$\propto \mathcal{A} \sum_{\epsilon=\pm 1} \frac{\Theta(\omega^2 - v_+^2 (k - \epsilon\pi)^2)}{\sqrt{\omega^2 - v_+^2 (k - \epsilon\pi)^2}^{2-1/K_+}} + \mathcal{B} \sum_{\epsilon, \epsilon'} \Theta \left[\omega^2 - v_+^2 \left(k - \pi \left(\frac{1}{2} - \epsilon' M \right) \right)^2 \right] \times \sqrt{\omega^2 - v_+^2 \left(k - \pi \left(\frac{1}{2} - \epsilon' M \right) \right)^2}^{2K_+ + 1/K_+ - 2} \quad (\text{F23})$$

$$\mathcal{I}^{(S^+_{-\omega, -k} S^-_{\omega, k})} = \text{gapped} \quad (\text{F23})$$

$$\mathcal{I}^{(\chi^z_{-\omega, -k} \chi^z_{\omega, k})} \propto \omega (\delta(\omega + v_+ k) + \delta(\omega - v_+ k)) \quad (\text{F24})$$

$$\mathcal{I}^{(S^z_{-\omega, -k} S^z_{\omega, k})} \propto \omega (\delta(\omega + v_+ k) + \delta(\omega - v_+ k)) \quad (\text{F25})$$

$$+ \sum_{\epsilon=\pm 1} \frac{\Theta(\omega^2 - v_+^2 (k - \epsilon\pi(\frac{1}{2} - M))^2)}{\sqrt{\omega^2 - v_+^2 (k - \epsilon\pi(\frac{1}{2} - M))^2}^{2-K_+}}$$

- in the vector chiral phase:

$$\mathcal{I}^{(\chi^z_{-\omega, -k} \chi^z_{\omega, k})} \quad (\text{F26})$$

$$\propto \mathcal{A} \omega^3 (\delta(\omega + v_+ k) + \delta(\omega - v_+ k)) + \mathcal{B} \sum_{\epsilon, \epsilon'=\pm 1} [\Theta(\omega^2 - v_+^2 (k - \epsilon 2\pi M - \epsilon' \pi)^2)] \times \sqrt{\omega^2 - v_+^2 (k - \epsilon 2\pi M - \epsilon' \pi)^2}^{4K_+ - 2} \quad (\text{F27})$$

$$\mathcal{I}^{(S^z_{-\omega, -k} S^z_{\omega, k})} \propto \omega (\delta(\omega + v_+ k) + \delta(\omega - v_+ k)) \quad (\text{F27})$$

$$\mathcal{I}^{(S^x_{-\omega, -k} S^x_{\omega, k})} \propto \sum_{\epsilon=\pm 1} \frac{\Theta(\omega^2 - v_+^2 (k - \epsilon Q)^2)}{\sqrt{\omega^2 - v_+^2 (k - \epsilon Q)^2}^{2-1/(4K_+)}}$$

$$\mathcal{I}^{((S^+ S^+)_{-\omega, -k} (S^+ S^+)_{\omega, k})} \quad (\text{F28})$$

$$\propto \sum_{\epsilon=\pm 1} \frac{\Theta(\omega^2 - v_+^2 (k - \epsilon 2Q)^2)}{\sqrt{\omega^2 - v_+^2 (k - \epsilon 2Q)^2}^{2-1/K_+}}.$$

In all the above, \mathcal{A} and \mathcal{B} are constants, and $Q = \frac{\pi}{2} - \frac{1}{2} \sqrt{\frac{\pi}{2}} \langle \partial_x \theta_+ \rangle$.

Note, in particular, that, since K increases monotonically between $1/2$ and 1 ($K(M=0) = 1/2$ and $K(M=1/2) = 1$), and $K_+ = K(1 + K \frac{J_1}{\pi v})$, $K_+ \geq 1/2$. Moreover, the bosonization approach is valid only “not too close” from the saturation limit $M = 1/2$, and in the weak coupling regime $v \sim J_2$. So, in particular:

$$\begin{cases} 2 - \frac{1}{K_+} \geq 3/2 \\ K_+ + \frac{1}{K_+} - 2 \geq 0 \\ 2 - K_+ \geq 0 \\ 4K_+ - 2 \geq 0 \\ 2 - \frac{1}{4K_+} \geq \frac{15}{8} \end{cases} \quad \text{if } K \leq \pi v \frac{-1 + \sqrt{1 + 8J_1/(\pi v)}}{2J_1}. \quad (\text{F29})$$

Note that $K \leq \pi v \frac{-1 + \sqrt{1 + 8J_1/(\pi v)}}{2J_1}$ is always true for $\frac{J_1}{\pi v} \leq 1$.